Vision Research 48 (2008) 1456–1470

Contents lists available at ScienceDirect

Vision Research

journal homepage: www.elsevier.com/locate/visres

Possible mechanisms underlying tilt aftereffect in the primary visual cortex: A critical analysis with the aid of simple computational models

Mauro Ursino *, Elisa Magosso, Cristiano Cuppini

Department of Electronics, Computer Science, and Systems, University of Bologna, viale Risorgimento 2, I-40136 Bologna, Italy

ARTICLE INFO

Article history:
Received 11 May 2007
Received in revised form 10 March 2008

Keywords:
Adaptation
Aftereffect
Neural computation
Excitation
Inhibition

ABSTRACT

A mathematical model of orientation selectivity in a single hypercolumn of the primary visual cortex developed in a previous work [Ursino, M., & La Cara, G.-E. (2004). Comparison of different models of orientation selectivity based on distinct intracortical inhibition rules. *Vision Research, 44*, 1641–1658] was used to analyze the possible mechanisms underlying tilt aftereffect (TAE). Two alternative models are considered, based on a different arrangement of intracortical inhibition (an *anti-phase model* in which inhibition is in phase opposition with excitation, and an *in-phase model* in which inhibition has the same phase arrangement as excitation but wider orientation selectivity). Different combinations of parameter changes were tested to explain TAE: a threshold increase in excitatory and inhibitory cortical neurons (fatigue), a decrease in intracortical excitation, an increase or a decrease in intracortical inhibition, a decrease in thalamo-cortical synapses. All synaptic changes were calculated on the basis of Hebbian (or anti-Hebbian) rules. Results demonstrated that the in-phase model accounts for several literature results with different combinations of parameter changes requiring: (i) a depressive mechanism to neurons with preferred orientation close to the adaptation orientation (fatigue of excitatory cortical neurons, and/or depression of thalamo-cortical synapses directed to excitatory neurons, and/or depression of intracortical excitatory synapses); (ii) a facilitatory mechanism to neurons with preferred orientation far from the adaptation orientation (fatigue of inhibitory cortical neurons, and/or depression of thalamo-cortical synapses directed to inhibitory neurons, and/or depression of intracortical inhibitory synapses). By contrast, the anti-phase model appeared less suitable to explain experimental data.

1. Introduction

A classic visual illusion is the tilt aftereffect (TAE). If a subject looks at an oriented stimulus (for instance, a grating with a given orientation) for a prolonged time, a subsequent stimulus with similar orientation appears rotated away from the adapting orientation. A common explanation for this phenomenon assumes that neurons in the primary visual cortex (V1) fatigue during prolonged activity. Since these neurons respond selectively to a particular orientation (Hubel & Wiesel, 1962), fatigue depends on the particular orientation used in the adapting period. These selective changes may explain the repulsive shift observed during the test phase.

However, results of recent physiological experiments performed on anesthetized cats revealed a more complex scenario (Dragoi, Sharma, & Sur, 2000). The tuning curve of V1 neurons exhibits depression near the adapting orientation (as assumed by the fatigue theory), but also the position of the peak response (i.e., the preferred orientation) repulsively shifts away from the adapting orientation. With a simple population coding model simulating the changes in the tuning curve of individual neurons in one hypercolumn, Jin, Dragoi, Sur, and Seung (2005) showed that suppression of the tuning curves contributes to the TAE, whereas the repulsive shift of the tuning curves reduces the amount of the TAE, and lessens the orientation error.

However, Jin et al.'s model (2005) did not investigate the possible physiological mechanisms responsible for the observed adaptation changes. In other words, the changes in the neuron tuning curves are described empirically in this model, without entering into possible mechanisms occurring in V1. Hence, a fundamental question remains open: which physiological adjustments induced by adaptation may explain the changes observed in neuron tuning curves, and the consequent TAE?

To answer this question, physiological models of the orientation selectivity in V1 able to incorporate the main currently known mechanisms must be used.

An important aspect to consider in these models is that neurons in V1 do not receive only an oriented input from the lateral geniculate nucleus, but also important connections (excitatory and inhibitory) from other cortical cells. As clearly documented in previous mathematical models of V1 (Ben-Yishai, Bar, & Sompolinsky, 1995; Carandini & Ringach, 1997; Somers, Nelson, & Sur, 1995;

* Corresponding author. Fax: +39 051 2093073.
E-mail address: mauro.ursino@unibo.it (M. Ursino).

0042-6989/$ - see front matter © 2008 Elsevier Ltd. All rights reserved.
doi:10.1016/j.visres.2008.04.002

Teich & Quian, 2006; Troyer, Krukowski, Priebe, & Miller, 1998; Ursino & La Cara, 2004) these intracortical connections improve the sharpness of the neuron orientation curve (i.e., they reduce the half width at half height of the tuning curve) and avoid the so-called "iceberg effect" (i.e., a progressive loss of orientation tuning when the contrast of the input image is increased) (Ferster & Milller, 2000). Since intracortical mechanisms play a fundamental role in determining the tuning curve of V1 cells, it is reasonable to expect that they are also involved in adaptation, and in the development of the consequent TAE.

According to the previous description, alternative scenarios have been proposed and different models presented to explain TAE in terms of physiological mechanisms. Some TAE models were based on the selective suppression of neural response, according to the fatigue hypothesis (Clifford, Wenderoth, & Spehar, 2000; Coltheart, 1971; Sutherland, 1961; Wainwright, 1999). A different plausible scenario involves adaptation of the excitatory connections to neurons tuned to the adapting orientation (Felsen et al., 2002; Teich & Quian, 2003). As a consequence of a reduced intracortical excitation, the response of these neurons would be diminished, resulting in the TAE. Lastly, a third scenario, especially explored by Bednar and Mikkulainen (2000), emphasizes the importance of inhibitory weight changes (i.e., an increase of inhibitory weights to neurons tuned for the adapting orientation). In this case, the activity of the neurons with preferred orientation proximal to the adapting orientation would be suppressed due to an increased intracortical inhibition by cortical interneurons. Furthermore, the involvement of a depression in inhibitory cortical synapses, and/or a depression in thalamo-cortical synapses in TAE cannot be ruled out.

Although different mechanisms may be responsible for the observed adaptation of V1 neurons to a grating, to our knowledge no quantitative study has compared the effect of the different hypotheses within a single theoretical framework. The situation is made even more complex by the existence of alternative hypotheses on the arrangement of intracortical inhibition, for instance inhibition in phase opposition with excitation [the so-called "push-pull model" (Teich & Quian, 2006; Troyer et al., 1998; Ursino & La Cara, 2004)] or inhibition in-phase with excitation but with a wider orientation tuning ("in-phase" model) (Somers et al., 1995; Teich & Quian, 2006; Ursino & La Cara, 2004). These two models probably do not behave in the same way, assuming a given adaptation of intracortical synapses.

In recent years we formulated some simple mathematical models of orientation selectivity in the primary visual cortex which include both the thalamic input and intracortical excitation and intracortical inhibition (either with "push-pull" or "in-phase" arrangement in two alternative models) (Ursino & La Cara, 2004). With suitable values of intracortical synapse parameters, these models mimicked experimental results quite well (before adaptation).

The aim of this work was to use the same models to investigate the possible physiological mechanisms responsible for adaptation in the primary visual cortex and the consequent TAE. This study specifically tested alternative hypotheses within the same model to allow immediate comparison of their consequences. In particular, fatigue of cortical neurons, changes in thalamo-cortical synapses and in intracortical synapses were implemented both in the "push-pull" and "in-phase" models, and their capacity to mimic real data checked vs. existing data in the literature. In addition, Hebbian (or anti-Hebbian) rules were used to modify synapses during the adaptation phase.

The present results and the models proposed may yield more insights into the mechanisms involved in visual adaptation for a quantitative critical examination of existing data, suggesting future experiments and additional hypotheses on TAE.

2. Method

Two different mathematical models were used in this work (in-phase and anti-phase) which differ as to the disposition of feedforward inhibition.

The models describe the output of neurons as a continuous quantity describing the firing rate. Both models consider the architecture of a single hypercolumn composed of 180 excitatory neurons and 45 inhibitory interneurons. Each neuron is parameterized by its preferred orientation, identified by the angle ϑ: two adjacent excitatory neurons differ in their preferred orientation by just 1°, while inhibitory interneurons differ by 4°. The ratio between the number of excitatory cells and inhibitory interneurons (180/45 = 4) is in agreement with the literature (Gabbott & Somogyi, 1986; McLaughlin, Shapley, Shelley, & Wielaard, 2000).

Equations of the model before adaptation are nearly identical to those presented in Ursino and La Cara (2004) where more details can be found. Equations for adaptation have never been presented before.

2.1. The response of geniculate cells

First the model describes the response of thalamic cells. The input to the thalamic cells is the intensity of light at the position (i,j) of the retina at time t (say $I(i,j,t)$). Since the cones in the retina are sensitive to local light intensity variations with respect to the average luminance (I_0), we consider a normalized luminance ($R(i,j,t)$) as follows:

$$R(i,j,t) = \frac{I(i,j,t) - I_0}{I_0} \tag{1}$$

We assume that thalamic cells have an ON center or an OFF center receptive field, described as the difference of two Gaussian functions. The input to a single LGN cell is computed as the dot product of the normalized luminance ($R(i,j)$ in Eq. (1)) and the receptive field. Lastly, the output of LGN cells is computed starting from the input by considering two non-linear effects: the output cannot decrease below zero, and exhibits progressive saturation if contrast approaches 0.3–0.35. In the following the output of an ON-center (or OFF-center) thalamic cell located at position x, y will be denoted with the symbol $T_{on}(x,y)$ (or $T_{off}(x,y)$).

Parameters were chosen to simulate the contrast response function of geniculate cells measured by Cheng, Chino, Smith, Hamamoto, and Yoshida (1995) using sinusoidal grating with spatial frequency 0.7 cyc/deg. The basal values have been given according to Troyer et al. (1998).

The values of all the parameters are reported in Table 1.

2.2. The thalamic input to ON-center simple cells

After having characterized the receptive field of a thalamic cell, we can construct the receptive field of excitatory (or inhibitory) cells in the primary visual cortex. These receptive fields are constructed using afferent inputs from 15 thalamic cells arranged in a regular lattice, oriented along the preferred orientation of the cell and sampled by means of a Gabor function (for more details, see Fig. 2 in Ursino & La Cara (2004)). The following expression for changes in membrane potential of an ON excitatory simple cell induced by its thalamic input can be written (see Ursino & La Cara, 2004 for more details):

$$\begin{aligned}\Delta V_{ct}^{ON}(\vartheta,t) = &\sum_{m=-2}^{+2} |w_{ct}(m\Delta x,0)| \cdot T_{on}(m\Delta x\cos\vartheta, -m\Delta x\sin\vartheta, t)\\ &+ \sum_{\substack{l=-1\\ l\neq 0}}^{+1}\sum_{m=-2}^{+2} |w_{ct}(m\Delta x, l\Delta y)| \cdot T_{off}(m\Delta x\cos\vartheta + l\Delta y\sin\vartheta,\\ &- m\Delta x\sin\vartheta + l\Delta y\cos\vartheta, t)\end{aligned} \tag{2}$$

where $\Delta V_{ct}^{ON}(\vartheta,t)$ represents the change in membrane potential of an excitatory cortical cell with preferred orientation ϑ caused by its thalamic input, Δx and Δy represent the distance between the centers of the thalamic cells in the preferred and

Table 1
Parameters of the models

W_{ct0}			0.02 mV/(spikes/s)	
W_{it0}			0.02 mV/(spikes/s)	
σ_x^2			0.49 deg^2	
σ_y^2			0.25 deg^2	
F			0.8 cyc/deg	
Δx			0.6°	
Δy			0.35°	
k_c			5 spikes/(s mV)	
υ			0.2 mV	
υ_1			0.2 mV	
τ			15 ms	
	W_{ex0}	σ_{ex}	W_{in0}	σ_{in}
Anti-phase	0.007 mV/(spikes/s)	0.0707	0.2 mV/(spikes/s)	0.0488
In-phase	0.018 mV/(spikes/s)	0.05	0.05 mV/(spikes/s)	0.4472

orthogonal orientations, respectively, $T_{on}(x,y,t)$ and $T_{off}(x,y,t)$ represent the activity, at the instant t, of an ON center or OFF center thalamic cell centered at position x, y. Finally, w_{ct} represents the synaptic strength from the thalamic cell to its target excitatory cortical cell. The absolute value has been used to have only excitatory connections from the thalamus to the cortex, in agreement with physiological knowledge. The expression for w_{ct} is

$$w_{ct} = w_{ct0} \cdot e^{-(x^2/\sigma_x^2)} \cdot e^{-(y^2/\sigma_y^2)} \cos(2\pi f y) \tag{3}$$

where parameters σ_x^2 and σ_y^2 set the dimension of the receptive field, and the spatial frequency, f, is correlated with the width of the ON and OFF subregions.

Equations similar to (2) and (3) were also used to calculate the thalamic input (say ΔV_{it}) to cortical inhibitory interneurons. The role of these neurons will be described below.

All the parameters in Eqs. (2) and (3) were assigned in acceptable accord with physiological data (Alonso, Usrey, & Reid, 2001; Cheng et al., 1995; Ferster, Chung, & Wheat, 1996; Gardner, Anzai, Ohzawa, & Freeman, 1999; Jones & Palmer, 1987a, 1987b; Reid & Alonso, 1995; Tanaka, 1983; Troyer et al., 1998) (see Table 1).

2.3. The intracortical circuitry

Two different models for intracortical connections have been used in this paper. These connections are identical to those used in the previous paper (Ursino & La Cara, 2004), hence only qualitative aspects are summarized in the following. Both models assume that intracortical excitation arrives from other excitatory neurons in the same hypercolumn whereas inhibition comes from inhibitory interneurons. Like the excitatory cells, inhibitory interneurons are parameterized by their orientation preference, and their activity is only a function of their thalamic input, i.e., these neurons do not receive intracortical synapses. As a consequence, intracortical inhibition to excitatory cells is arranged according to a feedforward scheme. By contrast, excitation involves a feedback among excitatory cortical cells. The corresponding dynamic is described via a differential equation with time constant τ.

The previous concepts are summarized by the following equations

$$\Delta V_c^{ON}(\vartheta,t) = \Delta V_{ct}^{ON}(\vartheta,t) + \Delta V_{ce}^{ON}(\vartheta,t) - \Delta V_{ci}^{ON}(\vartheta,t) \tag{4}$$

$$\tau \frac{dc^{ON}(\vartheta,t)}{dt} = -c^{ON}(\vartheta,t) + k_c \left[\Delta V_c^{ON}(\vartheta,t) - \upsilon\right]^+ \tag{5}$$

where $\Delta V_{ct}(\vartheta,t)$, $\Delta V_{ce}(\vartheta,t)$ and $\Delta V_{ci}(\vartheta,t)$ are the changes in membrane potential caused by the thalamic input (Eq. 2), and by the excitatory and inhibitory intracortical connections, respectively, $c(\theta,t)$ is the output activity of the cortical cell at time t, ϑ represents the orientation preference, υ is a threshold, and the symbol $[]^+$ denotes the positive part.

In both models the strength of excitatory and inhibitory cortical synapses decreases with the distance between the orientation preference of the presynaptic and postsynaptic cells. This decrease is mimicked via Gaussian relationships with assigned variance. Feedforward inhibition to a target excitatory cell in the first model, named "*anti-phase inhibition model*", is in phase opposition with the thalamic input to the same cell (for this reason, a similar model is also named "push-pull" (Troyer et al., 1998)). Anti-phase inhibition is realized assuming that inhibitory interneurons directed to an ON cortical cell have an OFF receptive field. In the second model, named "*in-phase inhibition model*", feedforward inhibition has the same spatial phase as the target neuron (ON vs. ON).

It is worth noting that in the anti-phase model the decrease in synaptic strength with orientation distance is similar for the excitatory and inhibitory synapses, and inhibition is stronger than excitation. By contrast, the in-phase model requires inhibition to be weaker than excitation but has much broader orientation tuning.

In the following, the expressions used for $\Delta V_{ce}(\theta,t)$ and $\Delta V_{ci}(\theta,t)$. Eq. (4) are given for the two models.

2.4. The anti-phase inhibition model

In this model, we assume that inhibitory interneurons directed to ON cortical cells have OFF receptive fields (Ferster & Milller, 2000). Hence, by denoting with $i^{OFF}(\phi)$ the activity of the inhibitory interneuron with orientation preference ϕ, we can write

$$i^{OFF}(\phi,t) = k_c \left[\Delta V_{it}^{OFF}(\phi,t) - \upsilon_1\right]^+ \tag{6}$$

where ΔV_{it}^{OFF} represents the thalamic input to the inhibitory interneuron with an OFF receptive field. This is computed with an equation similar to (2), but inverting the position of the ON and OFF thalamic cells, and using the symbol $w_{it}(x,y)$ to represent synapses from the thalamus to inhibitory interneurons. The latter have a Gabor function expression similar to Eq. (3)

ON simple cells receive excitatory connections from the other ON simple cells, and inhibitory connections from the OFF interneurons. Hence, the following expressions can be used to compute cortical input to the simple cell, to be used in Eq. (4)

$$\Delta V_{ce}^{ON}(\vartheta,t) = \sum_{\phi} w_{ex}(\vartheta,\phi) \cdot c^{ON}(\phi,t) \tag{7}$$

$$\Delta V_{ci}^{ON}(\vartheta,t) = \sum_{\phi} w_{in}(\vartheta,\phi) \cdot i^{OFF}(\phi,t) \tag{8}$$

where the symbols $w_{ex}(\vartheta,\phi)$ represent the excitatory synapse from a simple cell with orientation ϕ to a simple cell with orientation θ and the same spatial phase (ON vs. ON), and $w_{in}(\vartheta,\phi)$ represents the synapse from an inhibitory interneuron (orientation preference ϕ) to a simple cell (orientation preference ϑ) and opposite spatial phase (OFF vs. ON).

The strength of synapses depends on the distance in preferred orientation. This choice is implemented by assuming a Gaussian relationship. Hence, we have

$$w_{ex}(\vartheta,\phi) = w_{ex0} \cdot e^{-[\delta(\vartheta-\phi)^2/(2\sigma_{ex}^2)]} \tag{9}$$

$$w_{in}(\vartheta,\phi) = w_{in0} \cdot e^{-[\delta(\vartheta-\phi)^2/(2\sigma_{in}^2)]} \tag{10}$$

where the "orientation distance", δ, is computed as follows

$$\delta(\vartheta-\phi) = \begin{cases} |\vartheta-\phi|/90 & \text{if } |\vartheta-\phi| \leqslant 90^\circ \\ (180-|\vartheta-\phi|)/90 & \text{if } |\vartheta-\phi| \geqslant 90^\circ \end{cases} \tag{11}$$

where $w_{ex0}, w_{in0}, \sigma_{ex}^2$ and σ_{in}^2 are constant parameters, and $\delta(\vartheta-\phi)$ represents the distance between the preferred orientations, normalized between 0 (equal orientation), and 1 (orientation difference = 90°).

2.5. The in-phase inhibition model

In this model inhibitory interneurons receive only the thalamic input, but with a receptive field of the same phase as the cortical cells. Hence,

$$i^{ON}(\phi,t) = k_c \left[\Delta V_{it}^{ON}(\phi,t) - \upsilon_1\right]^+ \tag{12}$$

where ΔV_{it}^{ON} represents the thalamic input to the inhibitory interneuron with an ON receptive field. This is computed with an equation similar to (2) (still with an ON receptive field) but with thalamo-cortical synapses $w_{it}(x,y)$ from the thalamus to inhibitory interneurons.

The model is then completed by the following equations

$$\Delta V_{ce}^{ON}(\vartheta,t) = \sum_{\phi} w_{ex}(\vartheta,\phi) c^{ON}(\phi,t). \tag{13}$$

$$\Delta V_{ci}^{ON}(\vartheta,t) = \sum_{\phi} w_{in}(\vartheta,\phi) i^{ON}(\phi,t) \tag{14}$$

with expressions (9)–(11) for w_{ex} and w_{in} but different parameter values.

A list of parameter values is shown in Table 1 of the text.

2.6. The adaptation phase

In order to simulate adaptation, we assumed various different changes caused by prolonged activity of intracortical neurons: (i) a fatigue of excitatory neurons and/or inhibitory cortical neurons, (ii) a change in thalamo-cortical synapses; (iii) a depression of intracortical excitatory synapses, (iv) a change (either reinforcement or depression) in intracortical inhibitory synapses. In cases ii, iii and iv we adopted a classic Hebbian (or anti-Hebbian) adaptation rule.

To simplify the mathematical treatment, the adaptation phase and the test phase are considered in the following as completely separate, i.e., we first modify model parameters (adaptation phase) using the output of neurons in normal conditions, then we use the model with modified parameters to simulate its behavior in the test phase. Of course, this is a simplification (but commonly used in most neural network models) since, in reality, the outputs of neurons start to change during the adaptation phase.

The adaptation changes are mathematically described below:

2.7. Fatigue of cortical (excitatory and inhibitory) neurons

In order to simulate a simple fatigue phenomenon, we assumed that the threshold of excitatory cortical cells (that is, parameter υ in Eq. 5) and/or the threshold of inhibitory neurons (parameter υ_1 in Eq. (6) or Eq. (12)) increase in proportion to the activity of the neuron during the adaptation period. By denoting with $\Delta\upsilon$ a parameter establishing the adaptation strength, we can write:

$$\upsilon_{new}(\vartheta) = \upsilon + \Delta\upsilon \cdot \frac{c^{ON}(\vartheta,\infty)}{\max_\vartheta\{c^{ON}(\vartheta,\infty)\}} \tag{15}$$

where $c^{ON}(\vartheta,\infty)$ represents the output of the excitatory cell with preferred orientation ϑ during the adaptation period in steady state conditions (i.e., after the end of the transient period, $t \to \infty$) and $\upsilon_{new}(\vartheta)$ represents the new threshold of an excitatory cell with preferred orientation ϑ, after adaptation. Hence, the ratio $c^{ON}(\vartheta,\infty)/\max_\vartheta\{c^{ON}(\vartheta,\infty)\}$ represents the activity of neurons in the hypercolumn, normalized to the maximal activity during adaptation. Thanks to this normalization, parameter $\Delta\upsilon$ is equal to the threshold change in the neuron with maximal adaptation. Conditions characterized by more or less adaptation can be simulated by simply modifying this parameter (see Section 3).

An equation analogous to (15) was also applied to the threshold of inhibitory interneurons (parameter υ_1 in Eq. (6) or Eq. (12)). By denoting with $\Delta\upsilon_1$ a parameter setting the adaptation strength, we have

$$v_{1new}(\vartheta) = v_1 + \Delta v_1 \cdot \frac{i^{OFF}(\vartheta,\infty)}{\max_{\vartheta}\{i^{OFF}(\vartheta,\infty)\}} \quad \text{(anti-phase model)} \tag{16}$$

$$v_{1new}(\vartheta) = v_1 + \Delta v_1 \cdot \frac{i^{ON}(\vartheta,\infty)}{\max_{\vartheta}\{i^{ON}(\vartheta,\infty)\}} \quad \text{(in-phase model)} \tag{16'}$$

2.8. Depression of the excitatory synapses

In this rule we assumed that the synapses linking two excitatory cortical cells (i.e., the quantities $w_{ex}(\theta,\phi)$ in Eq. (9)) are modified via an anti-Hebbian rule: the *decrease* in synaptic strength depends on the correlation between the presynaptic and postsynaptic activity during the adaptation period. This decrease affects the parameter w_{ex0} in Eq. (9) (which was originally identical for all neurons). We can write:

$$w_{ex0,new}(\vartheta,\phi) = w_{ex0} + \Delta w_{ex0} \cdot \frac{c^{ON}(\vartheta,\infty)\cdot c^{ON}(\phi,\infty)}{\max_{\vartheta,\phi}\{c^{ON}(\vartheta,\infty)\cdot c^{ON}(\phi,\infty)\}} \tag{17}$$

where $w_{ex0,new}(\vartheta,\phi)$ is the new value of parameter w_{ex0} to be used in Eq. (9) for a synapse linking a presynaptic neuron with preferred orientation ϕ to a postsynaptic neuron with preferred orientation ϑ, Δw_{ex0} is a parameter which sets the strength of adaptation and the other quantities have the same meaning as in Eq. (15). In the following Δw_{ex0} is always held negative, i.e., we assumed that excitatory synapses can only be depressed due to adaptation. Thanks to normalization, Δw_{ex0} represents the maximum change in synapses during adaptation.

Hence, after adaptation, the excitatory synapse linking two neurons becomes:

$$w_{ex}(\vartheta,\phi) = w_{ex0,new}(\theta,\phi)\cdot e^{-\left[\delta(\vartheta-\phi)^2/(2\sigma_{ex}^2)\right]} \tag{18}$$

2.9. Changes (either reinforcement or depression) in inhibitory synapses

The third rule assumed that inhibitory synapses linking a presynaptic inhibitory cortical cell to a postsynaptic excitatory cell may change with a Hebbian (or anti-Hebbian) rule. The increase affects the parameter w_{in0} in Eq. (10) (which was originally identical for all neurons). We can write

$$w_{in0,new}(\vartheta,\phi) = w_{in0} + \Delta w_{in0} \cdot \frac{c^{ON}(\vartheta,\infty)\cdot i^{ON}(\phi,\infty)}{\max_{\vartheta,\phi}\{c^{ON}(\vartheta,\infty)\cdot i^{ON}(\phi,\infty)\}} \quad \text{(in-phase model)} \tag{19}$$

$$w_{in0,new}(\vartheta,\phi) = w_{in0} + \Delta w_{in0} \cdot \frac{c^{ON}(\vartheta,\infty)\cdot i^{OFF}(\phi,\infty)}{\max_{\vartheta,\phi}\{c^{ON}(\vartheta,\infty)\cdot i^{OFF}(\phi,\infty)\}} \quad \text{(anti-phase model)} \tag{19'}$$

where the first equation holds for the in-phase model [in which cortical cells receive in-phase inhibition, $i^{ON}(\varphi,\infty)$, from an interneuron with preferred orientation φ], and the second equation holds for the anti-phase model [in which cortical cells receive anti-phase inhibition, $i^{OFF}(\varphi,\infty)$, from an interneuron with preferred orientation φ but opposite (OFF vs. ON) receptive field]. Δw_{in0} is a parameter setting the strength of adaptation (we assume it can be either positive or negative), and the other quantities have the same meaning as in previous equations.

After application of the previous rule, the inhibitory synapse linking two neurons becomes:

$$w_{in}(\vartheta,\phi) = w_{in0,new}(\theta,\phi)\cdot e^{-\left[\delta(\vartheta-\phi)^2/(2\sigma_{in}^2)\right]} \tag{20}$$

2.10. Changes in thalamo-cortical synapses

As a last possibility, we also considered adaptation changes in thalamocortical synapses. The change affects the parameter w_{ct0} in Eq. (3) (which was originally identical for all neurons) and parameter w_{it0} (which has the same meaning as in Eq. (3), but concerns synapses from the thalamus to cortical interneurons). These parameters vary according to the correlation (or anticorrelation) of activity in the thalamic presynaptic cell and cortical postsynaptic cell.

Concerning a synapse linking a thalamic cell at position x, y to an excitatory cortical cell with preferred orientation ϑ, we can write

$$w_{ct0,new}(x,y,\vartheta) = w_{ct0} + \Delta w_{ct0} \cdot \frac{c^{ON}(\vartheta,\infty)\cdot T_{on/off}(x,y,\infty)}{\max_{\vartheta,x,y}\{c^{ON}(\vartheta,\infty)\cdot T_{on/off}(x,y,\infty)\}} \tag{21}$$

It is worth noting that the presynaptic thalamic cell can be ON if placed in the center region of the receptive field or OFF if placed in the peripheral region (see Eq. 2).

Similarly, concerning a synapse linking a thalamic cell at position x, y to an inhibitory cortical cell with preferred orientation ϑ

$$w_{it0,new}(x,y,\vartheta) = w_{it0} + \Delta w_{it0} \cdot \frac{i^{ON}(\vartheta,\infty)\cdot T_{on/off}(x,y,\infty)}{\max_{\vartheta,x,y}\{i^{ON}(\vartheta,\infty)\cdot T_{on/off}(x,y,\infty)\}} \quad \text{(in-phase model)} \tag{22}$$

$$w_{it0,new}(x,y,\vartheta) = w_{it0} + \Delta w_{it0} \cdot \frac{i^{OFF}(\vartheta,\infty)\cdot T_{off/on}(x,y,\infty)}{\max_{\vartheta,x,y}\{i^{OFF}(\vartheta,\infty)\cdot T_{off/on}(x,y,\infty)\}} \quad \text{(anti-phase model)} \tag{22'}$$

where, in the anti-phase model, the position of the ON or OFF thalamic cells is reversed.

2.11. Simulation of adaptation with different parameter changes

The adaptation phase consisted in the application of a grating with preferred orientation 80°, contrast 0.3 and spatial frequency 0.7 cyc/deg. According to our previous study, this value of contrast leads the thalamic cells close to saturation, while the spatial frequency is close to optimal for our simple cells (Ursino & La Cara, 2004). Different levels of adaptation were mimicked by assigning different values to the parameters Δv (threshold change of excitatory neurons, Eq. (15)), Δv_1 (threshold change of inhibitory interneurons, Eq. (16)), Δw_{ex0} (excitatory intracortical synapse change, Eq. (17)), Δw_{in0} (inhibitory intracortical synapse change, Eq. (19)), Δw_{ct0} and Δw_{it0} (changes in thalamo-cortical synapses to excitatory and inhibitory cortical neurons, Eqs. (21) and (22)) both for the in-phase and anti-phase models.

In the following, the threshold changes (Δv and Δv_1) will be expressed as absolute values, whereas the synaptic changes will be expressed as percentages of the presynaptic value.

After adaptation, a test phase was simulated by applying gratings with the same contrast and spatial frequency as the adapting grating (0.3 and 0.7 cyc/deg) and all possible orientations (from 1° to 180°). From these simulations, both the tuning curves (i.e., the neuron response to all 180 orientations), and the "population curve" (i.e., the response of all 180 neurons to a single orientation) could be computed.

An important problem is how the brain "reads out" the perceived orientation starting from the population curve. According to the literature (Pouget, Dayan, & Zemel, 2000; Vogels, 1990), different possibilities could be adopted. The present work tested four alternative metrics. The symbol ψ will be used in the following to represent the perceived orientation, and the subscript will distinguish the metrics.

(i) The winner takes all (WTA) metric. According to this solution, the perceived contrast is provided by the neuron with the maximum response; i.e.,

$$\psi_{WTA} = \mathrm{Max}_{\vartheta}\{c^{ON}(\vartheta,\infty)\} \tag{23}$$

(ii) The average value of the population curve (i.e., the barycentre). This is computed as follows

$$\psi_{bar} = \frac{\sum_{\vartheta=1}^{180} c^{ON}(\vartheta,\infty)\cdot\vartheta}{\sum_{\vartheta=1}^{180} c^{ON}(\vartheta,\infty)} \tag{24}$$

(iii) The population vector metrics (Georgopoulos, Kalaska, Caminiti, & Massey, 1982; Vogels, 1990), in which each neuron provides a two-dimensional vector, with its length equal to the firing rate and phase equal to twice its label. All these vectors are summed up, and the perceived orientation is taken as half the orientation of the final vector. Hence,

$$\psi_{vet} = \frac{1}{2}\mathrm{arctg}\left(\frac{\sum_{\vartheta=1}^{180} c^{ON}(\vartheta,\infty)\cdot\sin(2\vartheta)}{\sum_{\vartheta=1}^{180} c^{ON}(\vartheta,\infty)\cdot\cos(2\vartheta)}\right) \tag{25}$$

(iv) The maximum likelihood estimator (MLE), in which the population response is compared with a template, and the best-fit determines the perceived orientation. This work used a Gaussian function with free average value and standard deviation as a template, and we minimized a least-square criterion function of the difference between this Gaussian function and the population curve. The average value providing the optimal fit (say ψ_{MLE}) is assumed as the perceived orientation.

3. Results

In order to analyze the role of the different mechanisms on adaptation, a sensitivity analysis was performed using different combinations of parameter changes and testing their effects on physiological and psychophysical results. The following experimental aspects were checked:

(i) The value of TAE at moderate orientation differences (about 10°) between the test grating and the adaptation grating lie in the range 2°–7° (Dragoi et al., 2000).

(ii) The shift of the perceived orientation plotted vs. the orientation difference exhibits a positive peak (range 4°–7°) at small orientation difference (10°–30°) and falls to zero at about 45°. A mild negative value (−0.5°–1°, i.e., an indirect TAE) becomes visible at large orientation differences (60°–75°) (Bednar & Mikkulainen, 2000; Clifford et al., 2000; Jin et al., 2005)

(iii) The tuning curves of individual neurons exhibit a peculiar change after adaptation. After several minutes adaptation in cats, Dragoi et al. (2000) observed that the amplitude of the tuning curves decreases for neurons with preferred orientation close to the adapting one: the maximum reduction in amplitude can be over 40–45% [(Dragoi et al., 2000); see also (Jin et al., 2005)]. Neurons with distant preferred orientation exhibit an increase in their amplitude (about 15–25%).

(iv) The optimal orientation of the tuning curves of individual neurons exhibits a repulsive shift after several minutes adaptation in cats (range 2°–10°) (Dragoi et al., 2000; Dragoi, Sharma, Miller, & Sur, 2002). A repulsive shift in the tuning curves was also observed by Felsen et al. (2002) and Müller, Metha, Krauskopf, and Lennie (1999), using a much shorter time scale. In Felsen et al., however, the repulsive shift was about 2°–4°, and the decrease in amplitude just 10–15%. The shift observed by Müller et al. was just 1.5°.

In order to test the model's capability to mimic these results, we first performed simulations by varying several parameters in a large range, with an adaptation grating at 80°, and we computed the response of individual neurons to a single test grating with orientation 90°. Only those parameter combinations which satisfied criterion (i) (TAE ≅ 2°–7°), with at least one of the metrics adopted, were subjected to further analysis. For these specific combinations of parameters, which produce reasonable levels of TAE, we then computed the tuning curves of all neurons after adaptation (by using test gratings with all orientations between 1° and 180°) and we evaluated the aspects at points (ii–iv).

The results are reported in Tables 2 and 3 for the anti-phase and the in-phase models, respectively. Each row shows the parameter changes adopted, the percentage changes in the amplitude of the tuning curves after and before adaptation (maximum and minimum changes), the peak of the perceived orientation shift, i.e., the maximum direct TAE at small orientation differences (computed both with WTA, population vector and MLE metrics), the possible negative perceived orientation shift (i.e., an indirect aftereffect at large orientation differences, computed with the same metrics), and the maximum shift of the tuning curves (computed both with WTA and population vector metrics). The results of the barycentre metrics have not been shown, since they are close to the results of the population vector metric. Results of the MLE metric are not reported in the last column since they are almost indistinguishable from those of the population vector metric.

To clarify the previous results, Figs. 1–4 show some examples of the simulation curves with specific combinations of parameter changes paradigmatic of the behavior of the anti-phase and in-phase models. The figures display the tuning curves after adaptation (panel a), the shift in the preferred orientation of the tuning curves (panel b) and the perceived orientation shift (panel c) plotted vs. the orientation difference (using both the WTA and vector metrics as well as the MLE). Finally, the panels d and e investigate the effect of a progressive increase in parameter changes. To this end, eleven combinations of parameter changes were assigned: the population curves (panel d) and the TAE with a test grating at 90° (panel e) are presented for each combination.

Fig. 1 is an exemplum obtained with the anti-phase model, assuming that all parameters can change (i.e., this is the most complex adaptation). Some aspects of this figure deserve comment. First, as shown in Fig. 1a, the amplitude of the tuning curves at small orientation differences exhibits a moderate decrease (about −23%). However, the amplitude of tuning curves of neurons with a large orientation difference is unchanged. Second (Fig. 1b), the model predicts only a negligible repulsive shift in the preferred orientation of the individual neurons. Third (Fig. 1c), the perceived orientation shift (TAE) computed with the population vector and

Table 2
Effect of different parameter changes in the anti-phase model

	Trial	Δv	Δv_1	ΔW_{ex0} (%)	ΔW_{in0} (%)	ΔW_{ct0} (%)	ΔW_{it0} (%)	Amplitude ratio (Min–Max)	Max. direct TAE (°)	Indirect TAE (°)	Max. shift (°)
	1	0.8	0	0	0	0	0	82.05–100	9–2.8–3.0	0	0–0.2
	2	0.6	0.6	0	0	0	0	86.75–100	9–6.9–6.4	0	−1 to −0.2
	3	0	0	−12	0	0	0	89.14–100	6–0.9–1.2	0	0–0.2
	4	0	0	0	20	0	0	99.98–100	0	0	0
	5	0	0	−12	−12	0	0	89.15–100	6–0.9–1.2	0	0–0.2
	6	0	0	0	0	−4.2	0	87.0–100	6–1.4–1.6	0	1–0.3
	7	0	0	0	0	−3.5	3.5	89.21–100	5–0.7–0.9	0–0.1–0.1	1–0.44
	8	0	0	0	0	−4.2	4.2	87.06–100	6–0.8–1.1	0–0.1–0.1	1–0.5
	9	0	0	0	0	−3.5	−3.5	89.3–100	6–1.8–1.9	0	0–0.2
	10	0	0	0	0	−10	−10	69.3–100	13–5.9–6.2	0	1–0.7
	11	0	0	0	−24	−4	4	87.7–100	6–0.8–1.0	0–0.2–0.2	1–0.5
	12	0	0	−5	−5	−2.5	2.5	87.8–100	6–0.8–1.1	0	1–0.3
	13	0	0	−5	5	−2.5	2.5	87.4–100	6–0.8–1.1	0	1–0.4
	14	0	0	−10	−10	−10	−10	62.8–100.0	15–6.7–7.2	0	1–0.8
	15	0	0	−5	5	−2.5	2.5	87.4–100	6–0.8–1.1	0	1–0.4
Fig. 1	*16*	**0.5**	**0.5**	**−5**	**−5**	**−2.5**	**2.5**	**77.3–100.4**	**13–6.2–6.2**	**0**	**0–0.3**
	17	0.4	0.4	−4	−4	−2	−2	81.7–100.4	11–5.9–5.7	0	−1 to 0.2
	18	0.4	0.8	−12	−24	−4	4	70.3–100.5	16–9.2–9.0	0	0–0.5
	19	0.4	0.8	−4	−24	0	0	87.7–100.5	9–8.5–7.8	0	−1 to −0.2
	20	0.6	0.6	−24	−54	−2.4	2.4	63.6–100.5	18–8.7–8.9	0	0–0.4
	21	0.3	0.3	−12	−27	−1.2	−6.0	79.9–100.4	12–6.1–5.9	0	0–0.2

The parameter alterations are shown in the first six columns: absolute changes in the threshold of excitatory and inhibitory cortical neurons (first and second column), percentage changes in intracortical excitatory and inhibitory synapses (third and fourth column), percentage changes in excitatory and inhibitory thalamo-cortical synapses (fifth and sixth columns). Each row represents a different combination of parameter changes. The other columns represent: the minimum and maximum amplitudes of the tuning curves in percentage of normal (seventh column); the maximum repulsive TAE at small orientation differences, evaluated with the WTA, the vector method and the MLE (eighth column); the maximum indirect attractive aftereffect at large orientation differences, evaluated with the WTA, the vector method and the MLE (ninth column); the maximum repulsive shift in the preferred orientation of a neuron, evaluated with the WTA and the vector method (tenth column). Results of trial 16, emphasized in bold, are presented in Fig. 1.

Table 3
Effect of different parameter changes on the in-phase model

	Trial	Δv	Δv_1	ΔW_{ex0} (%)	ΔW_{in0} (%)	ΔW_{ct0} (%)	ΔW_{it0} (%)	Amplitude ratio (Min–Max)	Max. direct TAE (°)	Indirect TAE (°)	Max. shift (°)
	1	0.4	0	0	0	0	0	55.2–100.0	7–4.7–5.0	0	2–1.5
	2	0.5	0.5	0	0	0	0	94.1–139.5	8–5.5–5.5	1–0.3–0.4	1–1.3
	3	0.45	0.18	0	0	0	0	67.3–113.8	7–5.1–5.3	0–0.1–0.1	1–1.4
	4	0	0	−7	0	0	0	63.3–100.0	6–2.6–3.1	0	3–1.5
	5	0	0	0	14	0	0	54.9–100.0	7–4.5–4.9	0	2–1.7
	6	0	0	0	0	−3	0	55.8–100.1	7–4.0–4.5	0	3–2.0
	7	0	0	−10	10	0	0	36.9–100.0	11–6.0–6.9	0	4–2.7
	8	0	0	−8	−4	0	0	67.7–100.21	6–1.8–2.4	0–0.2–0.1	3–1.4
	9	0	0	−12	−28	0	0	94.7–109.9	4–0.1–0.1	4–4.6–3.7	2–0.5
	10	0	0	−15	−27	0	0	82.2–105.9	7–0–0	3–2.8–2.9	3–0.9
	11	0	0	−70	−70	0	0	43.7–103.3	18–0.4–3.8	2–5.9–3.4	5–1.9
	12	0.5	0	0	−2.5	0	0	52.1–100.0	7–5.1–5.4	0	2–1.6
	13	0	0	0	0	−4	−2	60.6–108.3	9–5.1–5.7	0–0.2–0.2	2–1.8
Fig. 4	**14**	**0**	**0**	**0**	**0**	**−5**	**−4**	**65.7–117.9**	**11–6.2–6.8**	**1–0.4–0.4**	**1–1.6**
	15	0	0	−1.8	1.8	−1.8	0	59.0–100.0	7–3.6–4.0	0	2–1.7
	16	0	0	−2.4	−2.4	−2.4	0	60.4–100.0	7–3.2–3.7	0	3–1.8
	17	0	0	−3	−7.5	−3	0	64.0–100.1	6–2.6–3.1	0	3–1.7
	18	0	0	−8	−16	−2	0	73.1–101.1	6–0.8–1.4	1–1.0–0.8	3–1.4
	19	0	0	−6	−12	−3	0	62.9–100.3	7–2.3–2.9	0–0.3–0.2	3–1.8
	20	0	0	−9	−21	−3	0	70.2–101.4	7–1.3–1.6	1–1.3–1.0	3–1.6
	21	0	0	−18	−56	−9	0	57.1–103.5	12–0.4–2.0	2–3.9–2.9	5–2.6
Fig. 2	**22**	**0.16**	**0.32**	**−8**	**0**	**0**	**0**	**67.8–125.5**	**10–4.9–5.6**	**0–0.3–0.4**	**3–2.2**
	23	0.2	0.2	0	10	0	0	66.5–115.4	8–5.2–5.5	0–0.2–0.2	2–1.7
	24	0.8	0.8	0	−12	0	0	123.5–164.5	7–5.4–5.3	1–0.1–0.4	1–0.8
	25	0.2	0.4	0	0	−2	0	88.1–131.9	7–4.5–4.7	1–0.3–0.4	2–1.6
	26	0.2	0.2	0	0	−2	0	67.8–115.5	8–4.8–5.1	0–0.2–0.2	2–1.8
	27	0.18	0.24	0	0	−2.4	0	68.2–118.7	8–5.1–5.4	0–0.2–0.2	2–2.0
	28	0	0	−4	−6	−4	0	45.2–100	9–4.8–5.6	0	4–2.6
	29	0	0	−4	−20	−4	0	79.19–101.3	5–0.5–1.0	1–1.0–0.9	3–1.2
	30	0	0	−14	−63	−12.6	0	52.2–103.4	13–0.9–2.6	2–3.7–2.8	7–3.3
	31	0	0	−6	0	−3	−3	56.3–113.2	11–5.8–6.6	0–0.3–0.3	2–1.9
	32	0.12	0.12	−6	−3	0	0	71.9–109.6	7–2.8–3.3	0–0.1–0.1	2–1.5
	33	0.08	0.24	−4	4	0	0	77.0–119.1	7–3.6–4.0	0–0.3–0.3	2–1.6
	34	0.14	0.42	−7	7	0	0	66.1–133.4	11–6.3–7.0	1–0.4–0.4	3–2.5
	35	0.08	0.16	−6	6	0	0	58.7–112.4	9–4.8–5.4	0–0.2–0.2	3–2.1
	36	0.21	0.21	−14	−7	0	0	53.9–116.6	12–5.0–6.1	0–0.3–0.3	4–2.4
Fig. 3	**37**	**0.28**	**0.28**	**−14**	**−7**	**0**	**0**	**53.2–122.2**	**12–5.9–7.0**	**0–0.3–0.3**	**4–2.6**
	38	0.08	0.16	0	8	−1.2	0	64.2–112.4	8–4.9–5.2	0–0.1–0.1	2–1.9
	39	0.21	0.21	0	0	−2.1	2.1	45.7–109.1	9–5.5–6.0	0	4–3.0
	40	0	0	−14	−63	−12.6	−6.3	66.0–136.1	17–3.0–5.6	2–4.0–3.0	4–2.2
	41	0.20	0.20	−2	−2.0	−1.2	0	73.7–115.0	7–3.9–4.3	0–0.2–0.2	1–2
	42	0.1	0.2	−7.5	−5	−2.5	0	53.11–115.8	11–5.4–6.3	0–0.2–0.2	4–2.7
	43	0.12	0.24	−9	−12	−3	0	57.9–119.4	11–4.8–5.8	0–0.4–0.4	4–2.7
	44	0.14	0.28	−21	−35	−7	0	39.3–123.0	16–6.3–8.7	1–1.0–0.8	6–4.0
	45	0.25	0.25	−2.5	−5	−1.25	0	77.5–119.8	7–3.9–4.2	0–0.2–0.3	2–1.5
	46	0.12	0.24	−9	−12	−3	−3	72.9–134.2	13–4.9–6.1	1–0.8–0.8	3–1.8
	47	0.2	0.4	−15	−20	−5	−5	61.1–156.3	19–7.9–10.7	1–1.2–1.1	3–2.4

The parameter alterations are shown in the first six columns: absolute changes in the threshold of excitatory and inhibitory cortical neurons (first and second column), percentage changes in intracortical excitatory and inhibitory synapses (third and fourth column), percentage changes in excitatory and inhibitory thalamo-cortical synapses (fifth and sixth columns). Each row represents a different combination of parameter changes. The other columns represent: the minimum and maximum amplitudes of the tuning curves in percentage of normal (seventh column); the maximum repulsive TAE at small orientation differences, evaluated with the WTA, the vector method and the MLE (eighth column); the maximum indirect attractive aftereffect at large orientation differences, evaluated with the WTA, the vector method and the MLE (ninth column); the maximum repulsive shift in the preferred orientation of a neuron, evaluated with the WTA and the vector method (tenth column). Results of trials 22, 37 and 14, emphasized in bold, are presented in Figs. 2–4.

MLE metrics is repulsive even at a large orientation difference, and the model does not produce an indirect TAE. These results are typical of all simulations performed with the anti-phase model, and disagree with experimental data.

The in-phase model provides better results, with various alternative combinations of parameter changes. Three different exempla are presented in Figs. 2–4. The case shown in Fig. 2 refers to fatigue in both excitatory and inhibitory cortical neurons, associated with an anti-Hebbian decrease in excitatory intracortical synapses. Fig. 3 assumes fatigue in excitatory and inhibitory neurons, together with anti-Hebbian decrease in both excitatory and inhibitory intracortical synapses. Finally, Fig. 4 assumes that adaptation occurs at the level of the thalamo-cortical synapses, by mimicking anti-Hebbian decrease in synapses from the thalamus to both excitatory and inhibitory cortical neurons.

It is worth noting that the results depicted in the last three figures are similar. The amplitude of individual tuning curves decreases at moderate orientation differences (the range is from −33% to −45%), and increases at large orientation differences (range from +14% to +25%) in all figures. The population curves (left bottom panels) show a clear distortion: consequently, the WTA method overestimates the perceived orientation shift. Normal values of TAE are provided by the other metrics. The curve "perceived shift vs. the orientation difference" obtained with these metrics (Figs. 2–4c) are in good agreement with the experimental data, and show a moderate indirect TAE at an orientation difference of 60°–70°. The repulsive shift in the preferred orientation of tuning curves (Figs. 2–4b) is about 2°–3°. Another interesting aspect is that a progressive increase in parameter changes causes a linear increase in the perceived TAE (Figs. 2–4e),

i.e., the model does not exhibit an intrinsic saturation in adaptation strength.

To shed more light on the intimate mechanisms responsible for the observed changes in the population curves and tuning curves, Fig. 5 displays the total inputs received by some neurons in two exemplary cases (trial no. 37, the same as in Fig. 3, and trial no. 14, the same as in Fig. 4). The upper panels show the thalamic input (i.e., quantity ΔV_{ci}^{ON} in Eq. (4)), the recurrent excitatory input (i.e., ΔV_{ce}^{ON} in Eq. (4)) and the inhibitory input ($-\Delta V_{ct}^{ON}$ in Eq. (4)) both before and after adaptation. The lower panels depict the total input changes (i.e., the difference in the quantity ΔV_{c}^{ON} after and before adaptation) to summarize the global effect. The three investigated neurons have preferred orientations of 90°, 105° and 120°.

Some conclusions can be drawn from these figures (similar conclusions can also be drawn from other simulations in Table 3, which are omitted for the sake of brevity). First, the greater input to the neurons is provided by the recurrent excitation, which, in the in-phase model, is about twice the thalamic input and twice the inhibition. Adaptation causes significant changes in the recurrent excitation, whereas adaptive changes in inhibition and thalamic input are smaller. Neurons with preferred orientation close to the adapting orientation show a significant decrease in their excitatory input close to the adapting orientation; neurons with preferred orientations far from the adapting orientation exhibit a significant excitation increase far from the adapting orientation. It is worth noting that the previous input changes are not symmetrical with respect to the preferred orientation of the neuron. For instance, for neurons with preferred orientation close to the adapting orientation, the excitatory input decreases slightly more in the proximal flank and less in the distal flank, thus resulting in a mild shift in the tuning curve. Neurons with preferred orientation at intermediate distance from the adapting orientation (range 100°–115°) exhibit a decrease in their input at the proximal flank and an increase in their input at the distal flank, with a clearer shift in the tuning curve.

In conclusion, the strong values of TAE are mainly due to the changes in the amplitude of the tuning curves (i.e., the amplitude decreases for proximal neurons and increases for distal neurons, thus resulting in a different population vector). Shift in the tuning curves can be ascribed to a moderate asymmetric input to neurons, mainly due to changes in recurrent excitation.

Finally, to establish a relationship between changes in tuning curves and adaptation effects, the results of Table 3 (in-phase model only) are summarized in the three panels of Fig. 6: they represent the peak TAE (i.e., the maximum perceived repulsive shift), the indirect TAE (i.e., the maximum perceived attractive shift, if present) and the maximum shift in the optimal orientation of individual neurons vs. the percentage alterations in the amplitude of the tuning curves. It can be seen that: (i) the peak TAE is correlated to the difference in the amplitude of the tuning curves at large and small orientation difference (panel a): the larger this difference, the larger the TAE. (ii) The shift in the optimal orientation of individual neurons (panel c) is correlated to the maximum decrease in the amplitude of the tuning curves. (iii) A good correlation is less evident for the indirect TAE (panel b): however, if unrealistic values of indirect TAE are excluded from the graph (for instance, values higher than 1.5°) a correlation can be found between the value of indirect TAE and the maximum increase in the amplitude of the tuning curves at large orientation difference.

4. Discussion

The present study analyzed the problem of adaptation to oriented gratings and TAE with the use of mathematical models including thalamic input and two alternative arrangements of intracortical synapses. Moreover, different possible mechanisms of adaptation were analyzed within the same theoretical framework.

The fundamental questions we set out to answer are: what is the arrangement of synapses, and what is the change in parameters (adaptation) which can best explain the experimental data summarized above? Which data cannot be explained by the model?

Looking at Table 3 and Figs. 2–4, we can say that the in-phase model can explain several results in the literature, but it requires at least two simultaneous parameter changes. By contrast, although the anti-phase model produces realistic values of TAE, it fails to mimic the other phenomena described above (such as the percentage changes in the amplitude of the tuning curves, the indirect TAE and the repulsive shift in the preferred orientation of individual neurons). In particular, the following relationships between parameter changes, alterations in the tuning curves, and adaptation can be construed:

(i) *Changes in the amplitude of the tuning curves.* In order to have a 40–50% decrease in the amplitude of the tuning curves at small orientation differences, it is necessary to assume the existence of a depressive mechanism (fatigue of cortical excitatory neurons, and/or depression of thalamo-cortical synapses directed to excitatory neurons, and/or depression of intracortical excitation). Moreover, to have a 10–20% increase in the amplitude of the tuning curves at large orientation differences, we need to partially suppress an inhibitory mechanism directed to excitatory neurons. This aspect can be readily implemented with the in-phase model, either by reducing the thalamic input to inhibitory interneurons, or reducing the inhibitory intracortical synapses, or assuming the fatigue of inhibitory cortical neurons. In fact, the in-phase model assumes that intracortical inhibition has broader tuning compared with excitation. By contrast, the anti-phase model cannot account for this effect since it assumes that inhibition has approximately the same tuning as excitation.

(ii) *The direct (repulsive) TAE.* There are many different combinations of parameter changes in both models which can produce values of TAE in agreement with experimental results, i.e., a repulsive shift in the perceived orientation as large as 4°–6° at moderate orientation differences between the adaptation and test gratings. It is worth noting that TAE values obtained with the barycentre and vector metrics are almost the same, but they slightly lower (about 0.5°) than the values computed with the MLE estimator. By contrast, the WTA metric provided values of TAE significantly exceeding those obtained with the other three metrics (this difference was often as large as 5°–6°).

In particular, with physiological changes in the tuning curves, the TAE was as large as 8°–11° with the WTA metrics, but approximately equal to 4°–6° with the other metrics. The reason for these differences is that the population curves are distorted by adaptation, hence the maximum of the population curve is significantly different from the average value. We claim that the use of the WTA metric induces values of TAE in excess compared with psychophysical data: probably the perceived orientation is read out by the brain using a vector population or a MLE method, while the WTA method appears less realistic.

Another important aspect clarified by our simulations is the dependence of TAE on the amplitude of the tuning curves. Results show that in the in-phase model TAE is directly correlated to the difference in the amplitude of the tuning curves at small and large orientation differences, rather than on the amplitude decrease only. In general, the higher this difference is, the higher the perceived repulsive shift. This

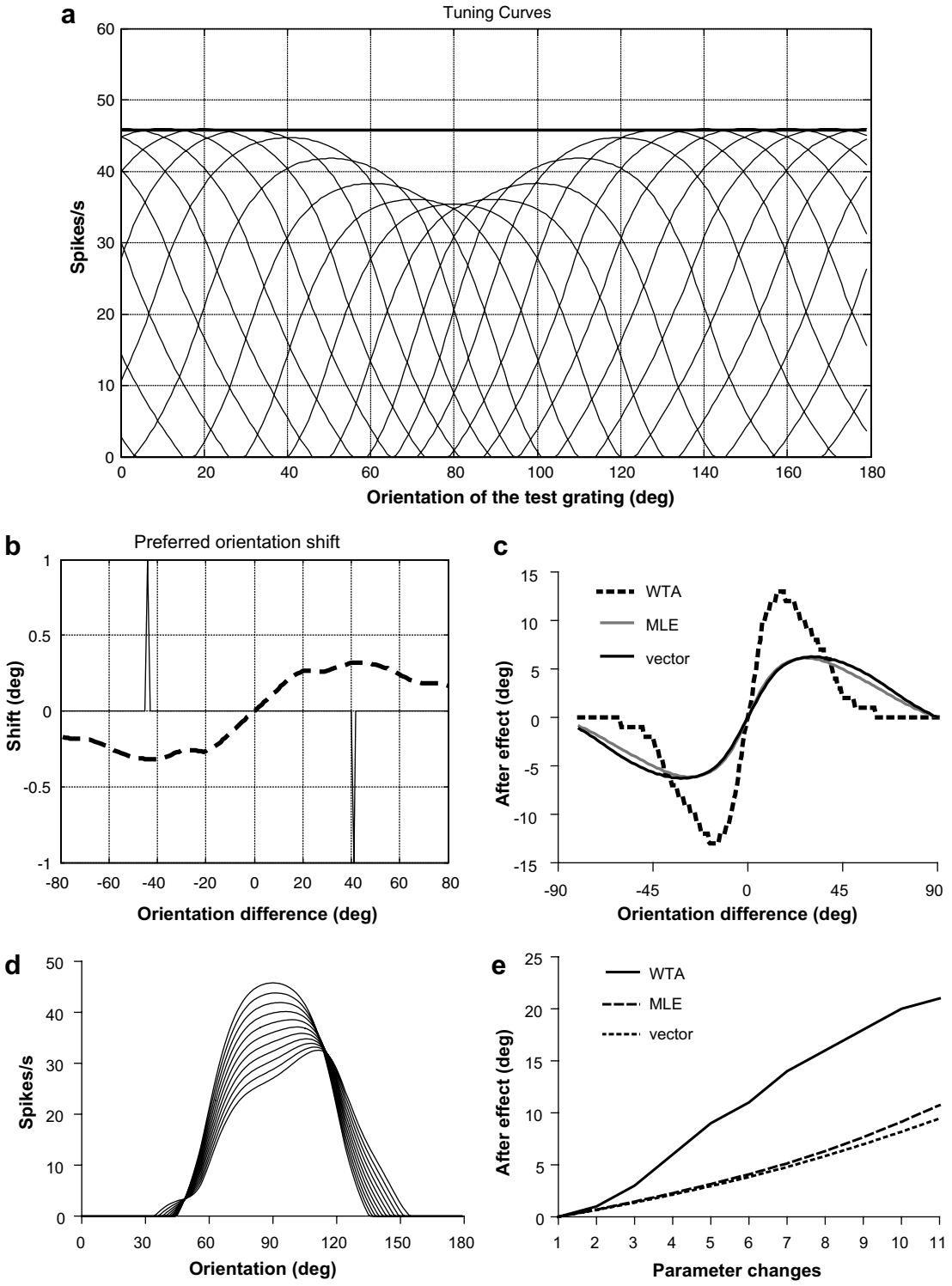

Fig. 1. An example of adaptation with different parameter changes in the anti-phase model. Panel (a) describes the tuning curves of several exemplary neurons (original preferred orientation between 0° and 180°, step 10°) after adaptation using the parameter changes as in *trial 16* of Table 2: increase in threshold of excitatory cortical neurons $\Delta\upsilon = 0.5$; increase in threshold of inhibitory cortical neurons: $\Delta\upsilon_1 = 0.5$; percentage changes in excitatory cortical synapses: $\Delta w_{ex0} = -5\%$; percentage changes in inhibitory cortical synapses: $\Delta w_{in0} = -5\%$; percentage changes in thalamo-cortical synapses to excitatory neurons: $\Delta w_{ct0} = -2.5\%$; percentage changes in thalamo-cortical synapses to inhibitory neurons: $\Delta w_{it0} = 2.5\%$. By comparison, the continuous thick line represents the basal amplitude (before adaptation) of all tuning curves. Panel (b) represents the shift in the preferred orientation of the tuning curves evaluated with the WTA method (i.e., the maximum of the tuning curve, thin line) and the population vector method (thick dashed line) and plotted vs. the orientation difference between the test grating and the adaptation grating. Panel (c) represents the apparent shift in perceived orientation evaluated from the population curves with the WTA metric (dashed line), the population vector metric (black continuous line) and the MLE (gray continuous line) and plotted vs. the orientation difference between the test grating and the adaptation grating. Panels (d) and (e) represent the population curves (d) and the apparent shift in perceived orientation (TAE) (e) evaluated at an orientation difference equal to 10° (test grating = 90°) by assuming a progressive increase in adaptation. To this end, adaptation was simulated by increasing each parameter within the range: $\Delta\upsilon = [0–1]$; $\Delta\upsilon_1 = [0–1]$; $\Delta w_{ex0} = [0\%$ to $-10\%]$; $\Delta w_{in0} = [0\%$ to $-10\%]$; $\Delta w_{ct0} = [0\%$ to $-5\%]$; $\Delta w_{it0} = [0–5\%]$. Each range was partitioned into 11 equal intervals, and adaptation was evaluated for each parameter at each interval. It is worth noting that simulations in panels (a–c) were performed exactly at the middle position of this partition. The TAE values were obtained with the WTA metric (continuous line), the vector metric (dotted line) and the MLE (dashed line).

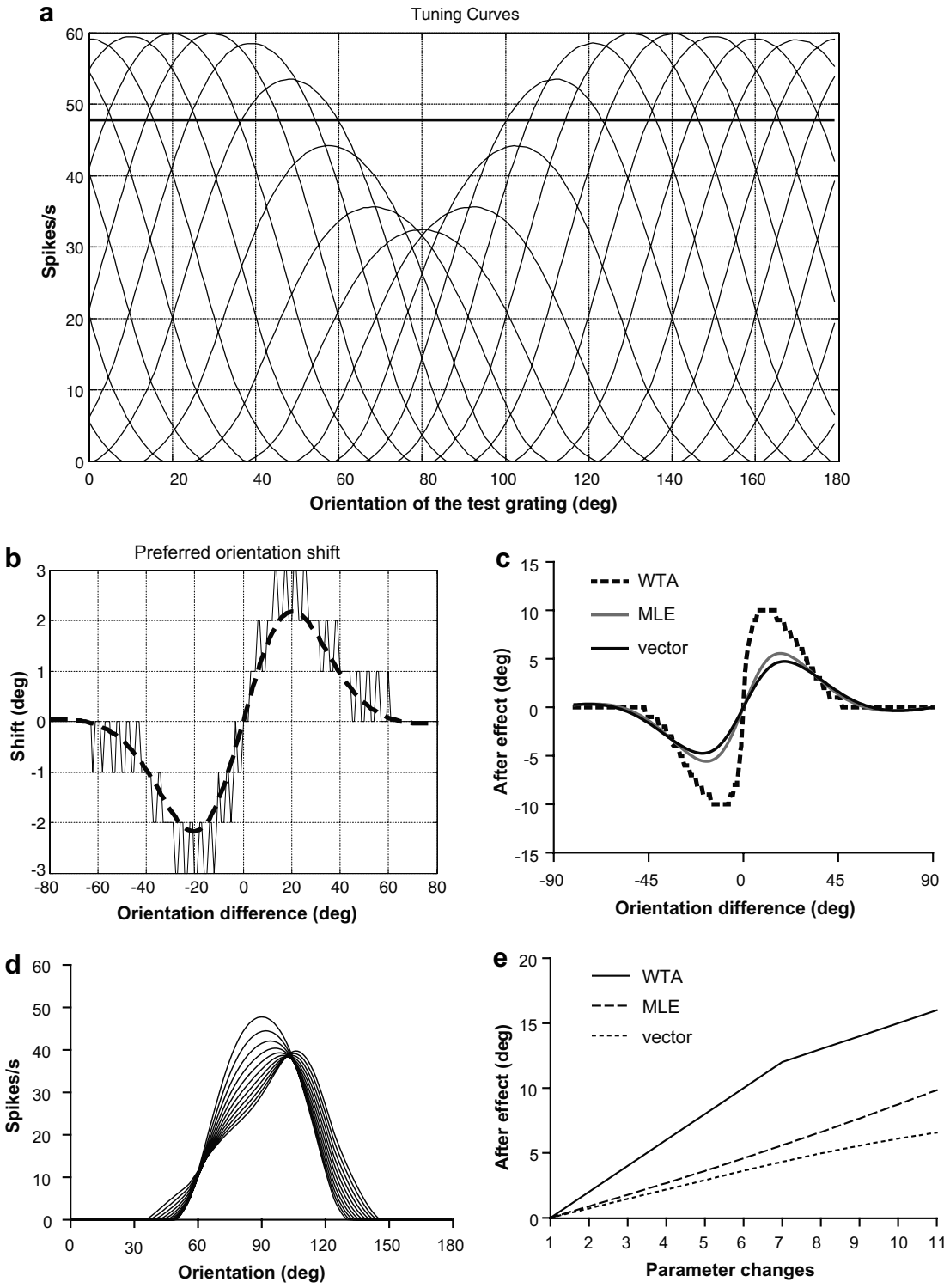

Fig. 2. An example of adaptation with different parameter changes in the in-phase model. The meaning of panels is the same as in Fig. 1. The assumed parameter changes were the same as in *trial 22* of Table 3: increase in threshold of excitatory cortical neurons $\Delta\upsilon = 0.16$; increase in threshold of inhibitory cortical neurons: $\Delta\upsilon_1 = 0.32$; percentage changes in excitatory cortical synapses: $\Delta w_{ex0} = -8\%$; percentage changes in inhibitory cortical synapses: $\Delta w_{in0} = 0$; percentage changes in thalamo-cortical synapses to excitatory neurons: $\Delta w_{ct0} = 0$; percentage changes in thalamo-cortical synapses to inhibitory neurons: $\Delta w_{it0} = 0$. To simulate increasing adaptation, parameters in the panels d and e were varied in the following range: $\Delta\upsilon = [0–0.32]$; $\Delta\upsilon_1 = [0–0.64]$; $\Delta w_{ex0} = [0\%$ to $-16\%]$; $\Delta w_{in0} = 0$; $\Delta w_{ct0} = 0$; $\Delta w_{it0} = 0$.

result signifies that TAE may be caused by a decrease in neuron input close to the adaptation orientation, further reinforced by input increase far from the adaptation orientation.

(iii) *The indirect (attractive) TAE*. The presence of an indirect aftereffect (i.e., a moderate attractive shift in the perceived orientation at large orientation differences) is directly correlated to the increase in the amplitude of the tuning curves. Hence, increase in neuron input with a consequent increase in the amplitude of the tuning curves far from the adaptation orientation seems the main determinant of this effect. According to this hypothesis, the anti-phase model, which does not predict an increase in the amplitude of the tuning

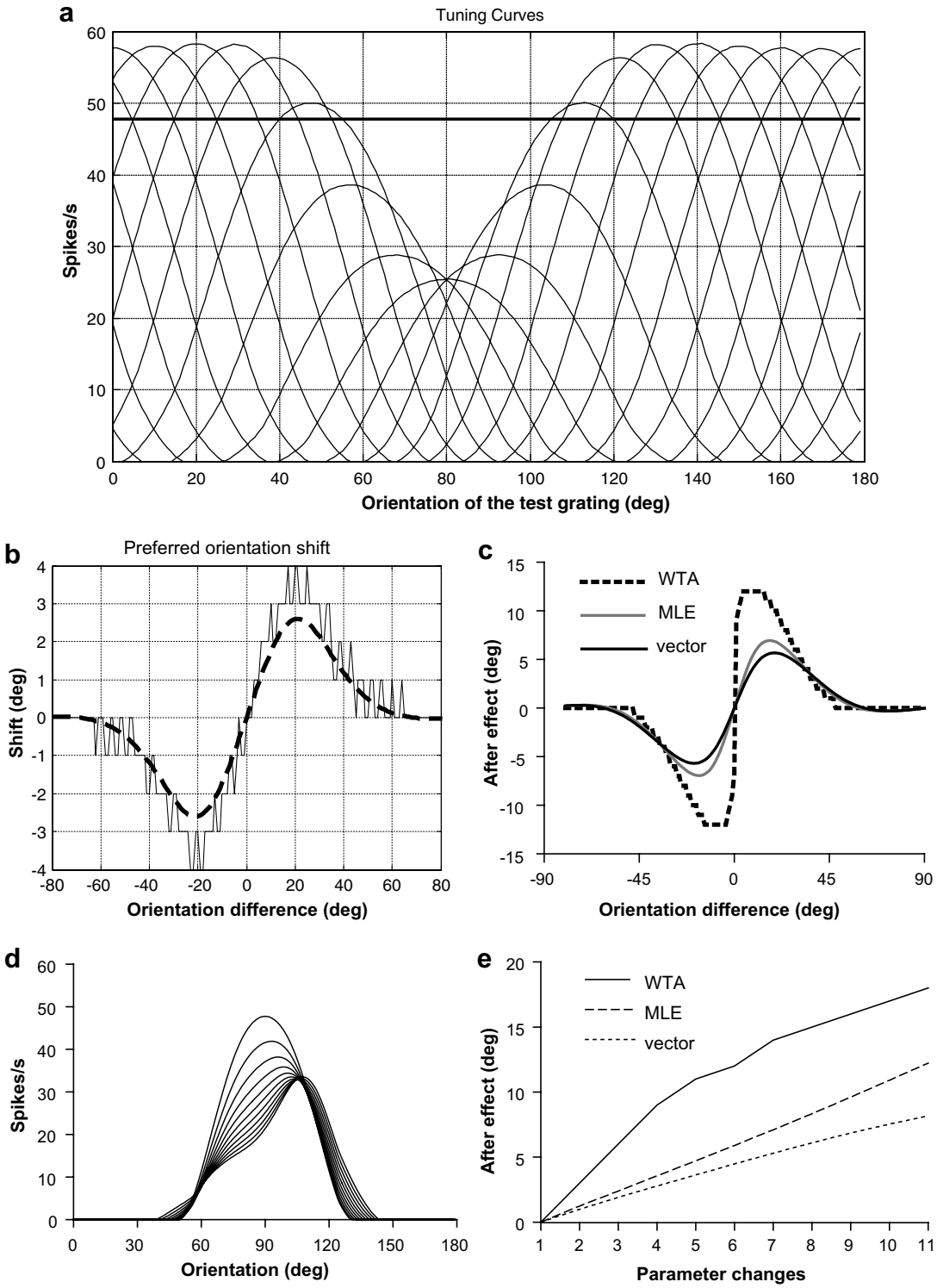

Fig. 3. An example of adaptation with different parameter changes in the in-phase model. The meaning of panels is the same as in Fig. 1. The assumed parameter changes were the same as in *trial 37* of Table 3: increase in threshold of excitatory cortical neurons $\Delta\upsilon = 0.28$; increase in threshold of inhibitory cortical neurons: $\Delta\upsilon_1 = 0.28$; percentage changes in excitatory cortical synapses: $\Delta w_{ex0} = -14\%$; percentage changes in inhibitory cortical synapses: $\Delta w_{in0} = -7\%$; percentage changes in thalamo-cortical synapses to excitatory neurons: $\Delta w_{ct0} = 0$; percentage changes in thalamo-cortical synapses to inhibitory neurons: $\Delta w_{it0} = 0$. To simulate increasing adaptation, parameters in the panels (d) and (e), were varied in the following range: $\Delta\upsilon = [0–0.56]$; $\Delta\upsilon_1 = [0–0.56]$; $\Delta w_{ex0} = [0\%$ to $-28\%]$; $\Delta w_{in0} = [0\%$ to $-14\%]$; $\Delta w_{ct0} = 0$; $\Delta w_{it0} = 0$.

curves, produces negligible values of the indirect TAE. It is worth noting that our conclusions agree with the results of Wenderoth and Smith (1999). Via experiments on volunteers, these authors, suggested that the direct TAE and the indirect TAE are mediated by different mechanisms.

(iv) *Repulsive shift in the preferred orientation of neurons*. The in-phase model predicts that the preferred orientation of individual neurons exhibits a repulsive shift after adaptation. The latter may be as large as 2°–4° in some cases reported in Table 3 (in-phase model) and is lower when computed

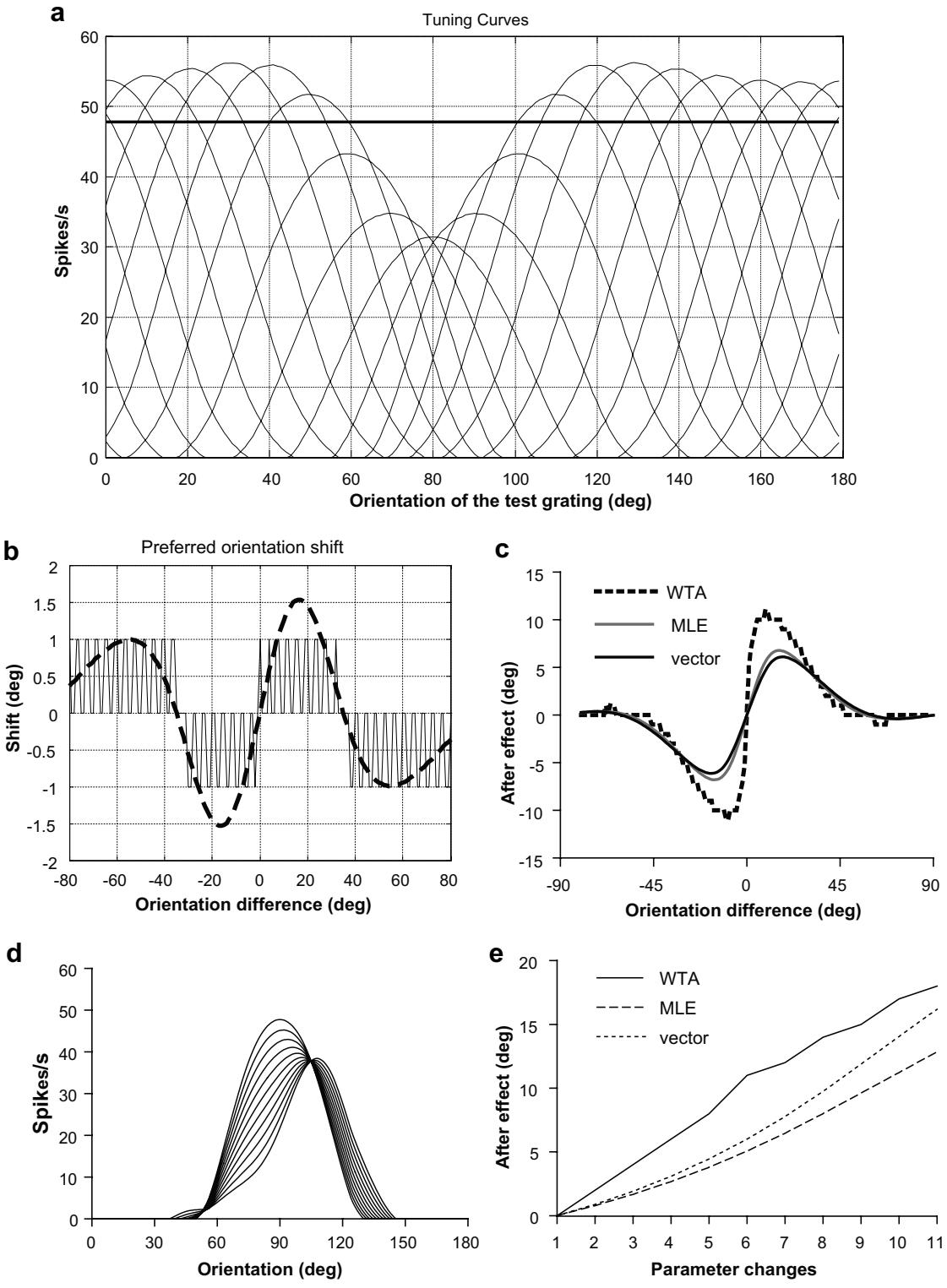

Fig. 4. An example of adaptation with different parameter changes in the in-phase model. The meaning of panels is the same as in Fig. 1. The assumed parameter changes were the same as in *trial 14* of Table 3: increase in threshold of excitatory cortical neurons $\Delta\upsilon = 0$; increase in threshold of inhibitory cortical neurons: $\Delta\upsilon_1 = 0$; percentage changes in excitatory cortical synapses: $\Delta w_{ex0} = 0$; percentage changes in inhibitory cortical synapses: $\Delta w_{in0} = 0$; percentage changes in thalamo-cortical synapses to excitatory neurons: $\Delta w_{ct0} = -5\%$; percentage changes in thalamo-cortical synapses to inhibitory neurons: $\Delta w_{it0} = -4\%$. To simulate increasing adaptation, parameters in the panels d and e, were varied in the following range: $\Delta\upsilon = 0$; $\Delta\upsilon_1 = 0$; $\Delta w_{ex0} = 0$; $\Delta w_{in0} = 0$; $\Delta w_{ct0} = [0\%$ to $-10\%]$; $\Delta w_{it0} = [0\%$ to $-8\%]$.

with the population vector method than with the WTA method. By contrast, the anti-phase model predicts only negligible values of the preferred orientation shift. The results of the in-phase model agree with values reported in some papers (Felsen et al., 2002; Müller et al., 1999). However, it is very difficult to simulate shift in preferred orientation as high as 10°–12°, as observed by Dragoi et al. (2000) in some cells. To obtain these values of shift magnitudes, we need to excessively decrease the amplitude of the tuning curves.

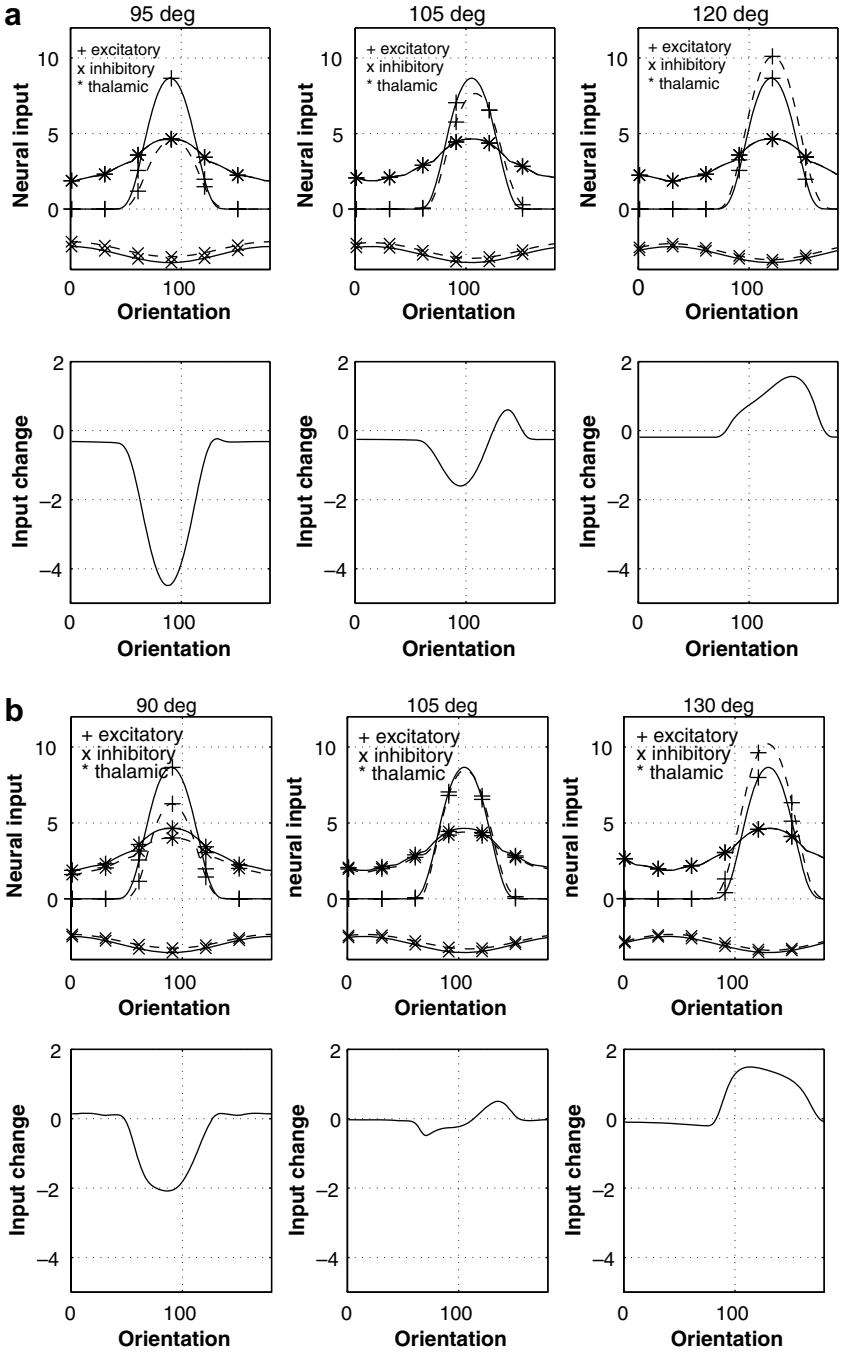

Fig. 5. (a) Input of a cortical neuron vs. stimulus orientation before and after adaptation, for three exemplary neurons (preferred orientation 90°, first column; 105°, second column; 120°, third columns). The assumed parameter changes were the same as in Fig. 3 (i.e., trial 37 of Table 3). The upper panels show the thalamic input (*), the excitatory input (+) and the inhibitory input (x) vs. orientation of the input stimulus before and after adaptation (continuous line and dotted line, respectively). The bottom panels show the postadaptation changes in neuron total input (i.e., the change of quantity ΔV_c^{ON} in Eq. (4) after adaptation). (b) The same simulation as in (a), but with the same parameters as in Fig. 4 (i.e., trial 14 of Table 3).

The preferred orientation shift seems correlated to a decrease in neuron response close to the adaptation orientation, whereas it seems quite independent of the amplitude increase far from the adaptation orientation. A qualitative exemplum is presented in Fig. 7 to explain the repulsive shift in preferred orientation. The continuous line in the figure represents the tuning curve of a neuron in the in-phase model, with a preferred orientation before adaptation equal to 90°. Further, we assumed that the response of the same neuron to different orientations is decreased after adaptation, but with a greater percentage decrease for orientations close to the adaptation orientation (80°) and a smaller percentage decrease for large orientation differences (see figure legend for mathematical details). As we can see, this non-uniform reduction in the response to oriented stimuli causes a repulsive shift in the preferred orientation. In our in-phase model, a non-uniform reduction in neuron response may be ascribed to a reduction in intracortical excitation (see Fig. 5). In fact, intracortical excitation coming from proximal neurons is maximally reduced when the input grating has the same orientation as the adaptation orientation. By contrast, the reduction in intracortical excitation in the anti-phase

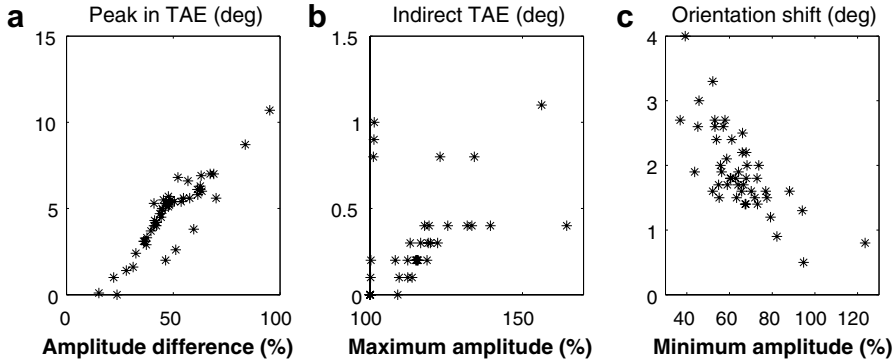

Fig. 6. Relationships between the changes in the amplitude of tuning curves and adaptation effects, obtained from results of Table 3 (in-phase model). (a) The peak of TAE (i.e., the maximum perceived repulsive shift) vs. the difference in amplitude of the tuning curves (i.e., the maximum amplitude minus the minimum amplitude, expressed as a percentage of normal amplitude). The correlation coefficient is: $\rho = 0.89$. (b) The indirect TAE (i.e., the maximum perceived attractive shift at large orientation differences) plotted vs. the maximum amplitude of the tuning curves, expressed as a percentage of normal. In drawing this figure, unrealistic values of indirect TAE (above 1.5°) have been omitted. The correlation coefficient is: $\rho = 0.48$. (c) The shift in the optimal orientation of individual neurons vs. the minimum amplitude of the tuning curves, expressed as a percentage of normal. The correlation coefficient is: $\rho = -0.72$. All results were computed with the MLE metric.

model is compensated by a similar reduction in intracortical inhibition, since both have a similar orientation tuning.

In summary, to reproduce physiological and psychophysical data on prolonged adaptation (Dragoi et al., 2000; Jin et al., 2005), at least two opposite mechanisms are required. First, one (or more) parameter changes are necessary to reduce the amplitude of the tuning curves close to the adapting orientation. This effect sharpens the tuning curves and, in the in-phase model, also induces a moderate repulsive shift of the preferred orientation. Second, one (or more) additional parameter changes should increase the amplitude far from the adapting orientation. This additional mechanism broadens the tuning curves and contributes to the indirect TAE. At present it is difficult to suggest which combinations of parameter changes better fit the experimental data. Figs. 2–4 show that several combinations are able to produce results in acceptable agreement with experimental data, both working on intracortical (Figs. 2 and 3) or thalamocortical (Fig. 4) mechanisms.

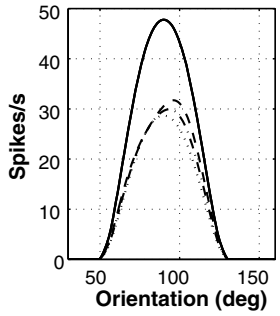

Fig. 7. A qualitative exemplum showing how adaptation can cause a repulsive shift in the preferred orientation of a neuron. The continuous line shows the tuning curve of a neuron with optimal orientation at 90° before adaptation. To qualitatively simulate adaptation, we assumed that the response of the neuron to a give orientation (say ϕ) is reduced by a constant factor plus a factor depending on the difference between the present orientation and the adaptation orientation (80°) which may mimic a decrease in intracortical excitation (which depends on the activity of other intracortical neurons, hence on the present orientation, ϕ. When ϕ is equal to the adaptation orientation, neurons' activity exhibits the maximum decrease). To simulate this phenomenon qualitatively, we calculated the tuning curve after adaptation with the following equation: $c_{after}(90,\phi) = c_{before}(90,\phi)\cdot[1-\Delta_1-\Delta_2\cdot\exp(-(80-\phi)^2/(2\sigma^2))]$ where c_{after} and c_{before} represent the neuron response after and before adaptation, the adaptation orientation is 80°, Δ_1 and Δ_2 are the strengths of the two reduction factors (the first independent of ϕ, the second dependent on the difference $80-\phi$). In all exempla, we used $\sigma = 15°$. Three exempla are shown, with $\Delta_1 = 0.4$ and $\Delta_2 = 0$ (dotted line), $\Delta_1 = 0.3$ and $\Delta_2 = 0.1$ (dash-dotted line) and $\Delta_1 = 0.2$ and $\Delta_2 = 0.2$ (dashed line). It is worth noting that the greater the second term, the greater the shift in preferred orientation.

4.1. Comparison with previous models

Many different models have been presented in recent years, with purposes similar to the present one (Bednar & Mikkulainen, 2000; Chelaru & Dragoi, 2008; Compte & Wang, 2006; Felsen et al., 2002; Jin et al., 2005; Schwabe & Obermayer, 2005; Teich & Quian, 2003).

Bednar and Mikkulainen (2000) used a physiological rule to simulate adaptation applying a Hebbian learning rule with normalization of synapses. Furthermore, they simultaneously applied this rule to all synapses in the model (both thalamic, excitatory intracortical and inhibitory). Hence, their simulations resemble the simulations reported in trials 46 and 47 of Table 3. Furthermore, they analyzed the behavior of many orientation columns and studied changes in orientation maps. The authors suggested that changes in inhibitory synapses are the main factors responsible for the observed TAE. Moreover, they also noticed a moderately attractive TAE with their model for orientation differences greater than 45°. However, the work by Bednar and Mikkulainen (2000) failed to investigate the amplitude and position of the tuning curves (an important test for any model of adaptation).

Felsen et al. (2002) analyzed the effect of rapid adaptation (on a very short time scale) using both a simple feedforward model (with thalamic input only) and a recurrent model (with intracortical connections) and showed that intracortical connection changes (in particular, a reduction in synaptic excitation) are necessary to have a consistent repulsive shift in the tuning curves. These authors did not use physiological adaptation rules.

Teich and Quian (2003), using a variation of the recurrent model by Carandini and Ringach (1997), distinguished between learning and adaptation. They suggested that a single parameter change (either a decrease in excitatory synapses or an increase in inhibitory synapses) can explain learning, whereas adaptation would require a combination of antagonistic changes. These changes may occur with a different time scale and, perhaps, with significant differences among animal species (Teich & Quian, 2003). Although we did not distinguish between learning and adaptation, several of our results agree with the considerations of Teich and Quian. A remarkable difference from our paper is that they did not use physiological rules for adaptation, nor did they analyze TAE vs. orientation difference. A further difference is that these authors suggested that adaptation cannot explain tilt aftereffect, since TAE would require

that "the tuning curves near the adapting orientation be shifted toward the adapted orientation". Our results demonstrate that TAE is also possible with a repulsive shift.

The latter problem was carefully analyzed by Jin et al. (2005). They explained many observations of the same group (Dragoi et al., 2000) with an empirical model in which tuning curves close to the adapting orientation reduce their amplitude while their preferred orientation is shifted away. Reduction in amplitude creates TAE, while the repulsive shift in preferred orientation reduces TAE. Although this work is an excellent summary of the phenomenological changes required to reproduce long-time adaptation, it does not enter into the physiological mechanisms involved.

Schwabe and Obermayer (2005) used a recurrent model of a visual hypercolumn with Hodgking–Huxley neurons to analyze the effect of alternative parameter changes (strength of afferent and recurrent synapses, neuronal gain, additive input) on the population response and tuning curves. According to their figures (namely Fig. 4 of their work) only adjusting recurrent synapses leads to results in good agreement with experimental data on adaptation (i.e., a repulsive shift in the orientation preference, a decrease in amplitude at the adapting orientation and an increase in amplitude far from the adapting orientation). A major difference between this work and ours is that they used an optimization criterion to modify parameters (based on Fisher information) instead of physiological rules.

Compte and Wang (2006), using a simple recurrent model, studied the shift in the receptive field position induced either by attention or adaptation (simulated by means of a positive or negative additive bias centered at a given position). Although this work focused on the spatial position of the stimulus, the same model can easily be generalized to alternative properties of the inputs, such as orientation. The authors observed that adaptation causes an attractive shift if intracortical inhibition dominates on excitation, and a repulsive shift if excitation dominates on inhibition. This result is similar to that obtained with our in-phase model by changing the threshold of neurons (in fact, in the in-phase model excitation locally dominates on inhibition).

An important study sharing several aspects with ours, was recently published (Chelaru & Dragoi, 2008). Using a recurrent model of interconnected populations of excitatory and inhibitory neurons, the authors examined the functional consequences of synaptic depression. Their main conclusion was that asymmetrical intracortical depression, in which excitatory synapses depress more than the inhibitory ones, causes a shift in the tuning curve, attenuation of neuron response to frequent stimuli and amplification of neuron response to infrequent stimuli. This result resembles that obtained with our model in some trials (see for instance trials 36 and 37) where we simultaneously depressed excitatory and inhibitory synapses. In particular, both models explain adaptation with a decrease in overall excitation close to the adapting stimulus, and an increase in input (increased excitation, decreased inhibition) far from the adapting stimulus. Two main differences, however, emerge between our results and those by Chelaru and Dragoi (2008). First, tuning curves in Chebaru and Dragoi exhibit larger shifts after adaptation. Second, the amplitude of their tuning curves decreases for neurons with preferred orientation close to the adapting orientation, but does not increase for neurons with preferred orientation far from the adapting orientation (whereas amplitude of our tuning curve increases at large orientation differences, in accordance with Dragoi et al. (2000)). These discrepancies might result from differences in model implementation. Chelaru and Dragoi used a learning rule which is based only on presynaptic activity, whereas we used the correlation between the presynaptic and postsynaptic activity (anti-Hebbian rule). Second, inhibition in their model is much higher than recurrent excitation (by a factor three) whereas in our model inhibition is much smaller than excitation. Lastly, we did not include recurrent inhibition in our model (our model inhibition is feedforward in type). It is possible that the use of recurrent inhibition may enhance inhibition depression, thereby resulting in a greater shift of the tuning curves (see Fig. 5G in Chelaru & Dragoi (2008)).

5. Conclusions

Although a few previous models anticipated some of our results, we claim that the present work adds two major new conclusions, which cannot be found elsewhere.

(i) By comparing the results of the in-phase and anti-phase models in identical conditions, we demonstrated that the anti-phase model cannot reproduce many aspects of adaptation observed experimentally. Since the debate between the two models remains open, this result is of value and provides a serious indication in favor of the in-phase model, at least for the cat's visual cortex where adaptation was investigated (Dragoi et al., 2000).

(ii) We demonstrate that adaptation can be achieved by a variety of possible mechanisms provided the structure of intracortical feedback is the same. Our conclusion is that adaptation is the effect of an initial bias in neuron inputs (excitation minus inhibition) induced by different combinations of parameter changes. This bias is then amplified by intracortical feedback which further attenuates the neuron output at the adapting orientation and reinforces neuron output at large orientation differences with a competitive mechanism. Hence, the structure of the intracortical recurrent mechanism is more essential to adaptation than the initial parameter change.

References

Alonso, J. M., Usrey, W. M., & Reid, R. C. (2001). Rules of connectivity between geniculate cells and simple cells in cat primary visual cortex. *The Journal of Neuroscience, 21*, 4002–4015.

Bednar, J., & Mikkulainen, R. (2000). Tilt aftereffects in a self-organizing model of the primary visual cortex. *Neural Computation, 12*, 1721–1740.

Ben-Yishai, R., Bar, O., & Sompolinsky, H. (1995). Theory of orientation tuning in visual cortex. *Proceedings of the National Academy of Sciences of the United States of America, 92*, 3844–3848.

Carandini, M., & Ringach, D. (1997). Predictions of a recurrent model of orientation selectivity. *Vision Research, 37*, 3061–3071.

Chelaru, M. I., & Dragoi, V. (2008). Asymmetric synaptic depression in cortical networks. *Cerebral Cortex, 18*, 771–788.

Cheng, H., Chino, Y., Smith, EL., Hamamoto, J., & Yoshida, K. (1995). Transfer characteristics of lateral geniculate nucleus X neurons in the cat: Effects of spatial frequency and contrast. *Journal of Neurophysiology, 74*, 2548–2557.

Clifford, CW., Wenderoth, P., & Spehar, B. (2000). A functional angle on some aftereffects in cortical vision. *Proceedings of the Royal Society of London. Series B. Biological Sciences, 267*, 1705–1710.

Coltheart, M. (1971). Visual feature-analyzers and the aftereffects of tilt and curvature. *Psychological Review, 78*, 114–121.

Compte, A., & Wang, X. J. (2006). Tuning curve shift by attention modulation in cortical neurons: A computational study of its mechanisms. *Cerebral Cortex, 16*, 761–778.

Dragoi, V., Sharma, J., Miller, EK., & Sur, M. (2002). Dynamics of neuronal sensitivity in visual cortex and local feature discrimination. *Nature Neuroscience, 5*, 883–891.

Dragoi, V., Sharma, J., & Sur, M. (2000). Adaptation-induced plasticity of orientation tuning in adult visual cortex. *Neuron, 28*, 287–298.

Felsen, G., Shen, Y. S., Yao, H., Spor, G., Li, C., & Dan, Y. (2002). Dynamic modification of cortical orientation tuning mediated by recurrent connections. *Neuron, 35*, 945–954.

Ferster, D., Chung, S., & Wheat, H. (1996). Orientation selectivity of thalamic input to simple cells of cat visual cortex. *Nature, 380*, 249–252.

Ferster, D., & Millller, K. (2000). Neural mechanisms of orientation selectivity in the visual cortex. *Neuroscience, 23*, 441–471.

Gabbott, P. L., & Somogyi, P. (1986). Quantitative distribution of GABA-immunoreactive neurons in the visual cortex (area 17) of the cat. *Experimental Brain Research, 61*, 323–331.

Gardner, J. L., Anzai, A., Ohzawa, I., & Freeman, R. D. (1999). Linear and nonlinear contributions to orientation tuning of simple cells in the cat's striate cortex. *Visual Neuroscience, 16*, 1115–1121.

Georgopoulos, A. P., Kalaska, J. F., Caminiti, R., & Massey, J. T. (1982). On the relations between the direction of two-dimensional arm movements and cell discharge in primate motor cortex. *The Journal of Neuroscience, 2*, 1527–1537.

Hubel, D., & Wiesel, T. N. (1962). Receptive fields, binocular interaction and functional architecture in the cat's visual cortex. *The Journal of Physiology, 160*, 106–154.

Jin, DZ., Dragoi, V., Sur, M., & Seung, S. (2005). The tilt aftereffect and adaptation-induced changes in orientation tuning in visual cortex. *Neurophysiology, 94*, 4038–4050.

Jones, J. P., & Palmer, L. A. (1987a). An evaluation of the two-dimensional Gabor filter model of simple receptive fields in cat striate cortex. *Journal of Neurophysiology, 58*, 1233–1258.

Jones, J. P., & Palmer, L. A. (1987b). The two-dimensional spatial structure of simple receptive fields in cat striate cortex. *Journal of Neurophysiology, 58*, 1187–1211.

McLaughlin, D., Shapley, R., Shelley, M., & Wielaard, D. J. (2000). A neuronal network model of macaque primary visual cortex (V1): Orientation selectivity and dynamics in the input layer 4Calpha. *Proceedings of the National Academy of Sciences of the United States of America, 97*, 8087–8092.

Müller, J. R., Metha, A. B., Krauskopf, J., & Lennie, P. (1999). Rapid adaptation in visual cortex to the structure of images. *Science, 285*, 1405–1408.

Pouget, A., Dayan, P., & Zemel, R. (2000). Information processing with population codes. *Nature Reviews. Neuroscience, 1*, 125–132.

Reid, RC., & Alonso, J. (1995). Specificity of monosynaptic connections from thalamus to visual cortical neurons in vitro. *Nature, 378*, 281–284.

Schwabe, L., & Obermayer, K. (2005). Adaptivity of tuning functions in a generic recurrent network model of a cortical hypercolumn. *The Journal of Neuroscience, 25*, 3323–3332.

Somers, D., Nelson, SB., & Sur, M. (1995). An emergent model of orientation selectivity in cat visual cortical simple cells. *The Journal of Neuroscience, 15*, 5448–5465.

Sutherland, N. (1961). Figural after-effects and apparent size. *Science, 13*, 222–228.

Tanaka, K. (1983). Cross-correlation analysis of geniculostriate neuronal relationships in cats. *Journal of Neurophysiology, 49*, 1303–1318.

Teich, AF., & Quian, N. (2003). Learning and adaptation in recurrent model V1 orientation selectivity. *Neurophysiology, 89*, 2086–2100.

Teich, AF., & Quian, N. (2006). Comparison among some models of orientation selectivity. *Journal of Neurophysiology, 96*, 404–419.

Troyer, TW., Krukowski, AE., Priebe, N., & Miller, K. (1998). Contrast-invariant orientation tuning in cat visual cortex: Thalamocortical input tuning and correlation-based intracortical connectivity. *The Journal of Neuroscience, 18*, 5908–5927.

Ursino, M., & La Cara, G.-E. (2004). Comparison of different models of orientation selectivity based on distinct intracortical inhibition rules. *Vision Research, 44*, 1641–1658.

Vogels, R. (1990). Population coding of stimulus orientation by striate cortical cells. *Biological Cybernetics, 64*, 25–31.

Wainwright, M. (1999). Visual adaptation as optimal information transmission. *Vision Research, 39*, 3960–3974.

Wenderoth, P., & Smith, S. (1999). Neural substrates of the tilt illusion. *Australian and New Zealand Journal of Ophtalmology, 27*, 271–274.